Utz von Wagner, Lukas Lentz

On Artifacts in Nonlinear Dynamics

von Wagner, Utz; Lentz, Lukas (2017): On Artifacts in Nonlinear Dynamics. In: Awrejcewicz, J.; Kaźmierczak, M.; Mrozowski, J.; Olejnik, P. (Eds.): Vibration, Control and Stability of Dynamical Systems (DSTA 2017), vol. 1, pp. 525–536. Proceedings DOI: https://doi.org/10.34658/9788393531257

On Artifacts in Nonlinear Dynamics

Utz von Wagner, Lukas Lentz

Abstract: Nonlinear oscillations are of permanent interest in the field of dynamics of mechanical and mechatronical systems. There exist several well-known semi-analytical methods like Harmonic Balance, perturbation analysis or multiple scales for such problems. We reconsider in our presentation the method of Harmonic Balance but add some additional steps in order to avoid artifacts and get information about the stability. The classical method of Harmonic Balance is therefore added by an error criterion, which considers the neglected terms. Looking on this error for increasing ansatz orders, it can be decided whether a solution exists or is an artifact of the method. For the low error solutions, a stability analysis is performed. As example, an extended Duffing oscillator with additional nonlinear damping and excitation is considered showing regions of separated island solutions. Also a nonlinear piezo-beam energy harvesting system is investigated. The described method enables to calculate solutions in a rapid manner with comparable low effort, to get an overview over regular responses of nonlinear systems.

1. Introduction

One of the most used academic examples for an oscillator in nonlinear dynamics is the so-called Duffing oscillator named after the German engineer Georg Duffing (1861-1944), who investigated in his original work 1918 an oscillator with quadratic and cubic stiffness and linear viscous damping performing free or forced harmonic vibrations [3]. Nowadays the term Duffing equation is used much broader and in general describes any nonlinear equation of motion including a cubic stiffness term. For solving such equations the method of Harmonic Balance was and is still very popular and described in many textbooks, e.g. by Hagedorn [2]. In the present paper an overview is given over some examples, where this method is extended by a corresponding error criterion introduced by Urabe et al. [7]. The examples are classical and extended Duffing oscillators added by an energy harvesting system.

2. Classical Duffing oscillator

Corresponding results for the classical softening Duffing oscillator are already described by the authors of the present paper in [9], where additionally to the Harmonic Balance an error criterion is applied which was also used much earlier by Urabe et al. [7]. This classical

softening Duffing oscillator is used in the present paper as well for introducing the method and showing some additional results compared to [9].

The Duffing oscillator is given by

$$m\ddot{x} + d\dot{x} + cx + \alpha x^3 = F_0 \cos \Omega t \tag{1}$$

with m being the oscillator mass, d the damping coefficient, c the linear stiffness, α the coefficient of the nonlinear stiffness, F_0 the excitation force amplitude and Ω the circular excitation frequency. In the case of the softening Duffing oscillator α is negative, while m, d, c and F_0 are positive. This equation is transformed with respect to dimensionless time derivatives by introducing the circular frequency of the undamped free linear vibrations $\omega_0^2 = c/m$, the damping ratio $D = d/(2\sqrt{cm})$ and the dimensionless time $\tau = \omega_0 t$ as

$$x''(\tau) + 2Dx'(\tau) + x(\tau) + \varepsilon x^3(\tau) = f \cos(\eta\tau) \tag{2}$$

with $()' = \mathrm{d}()/\mathrm{d}\tau$, $\varepsilon = \alpha/(m\omega_0^2)$, $f = F_0/(m\omega_0^2)$ and $\eta = \Omega/\omega_0$. Equation (2) is solved approximately by introducing the Harmonic Balance ansatz

$$x(\tau) = \sum_{k=1}^{n} \left(a_k \cos(k\eta\tau) + b_k \sin(k\eta\tau)\right). \tag{3}$$

Using the classical method of Harmonic Balance i.e. introducing (3) into (2) results in a system of nonlinear algebraic equations

$$\sum_{k=1}^{n} \left(\tilde{a}_k \cos(k\eta\tau) + \tilde{b}_k \sin(k\eta\tau)\right) = f \cos(\eta\tau) - \sum_{k=n+1}^{3n} \left(\tilde{a}_k \cos(k\eta\tau) + \tilde{b}_k \sin(k\eta\tau)\right). \tag{4}$$

Herein the coefficients $\tilde{a}_k,\ \tilde{b}_k$ are nonlinear functions of the original ansatz coefficients $a_k,\ b_k$. Following Harmonic Balance, the higher order frequency terms

$$\sum_{k=n+1}^{3n} \left(\tilde{a}_k \cos(k\eta\tau) + \tilde{b}_k \sin(k\eta\tau)\right) \tag{5}$$

in (4) are neglected. After this neglection the coefficients $a_k,\ b_k$ can be calculated from the modified equation (4).

For the visualization of the thereby determined approximate solution $x(\tau)$, $\hat{x}$ is defined as

$$\hat{x} = \max_{0 \le \tau \le \frac{2\pi}{\eta}} \left\{ \sum_{k=1}^{n} \left(a_k \cos(k\eta\tau) + b_k \sin(k\eta\tau)\right) \right\}. \tag{6}$$

Now as mentioned before an error criterion is introduced by considering the neglected terms in the Harmonic Balance method ([7], [9], [10]). The corresponding coefficients $\tilde{a}_k, \tilde{b}_k$ of the

neglected higher order terms can be calculated using the solution for a_k, b_k and the error $\hat{e}$ is defined from this by

$$\hat{e} = \max_{0 \le \tau \le \frac{2\pi}{\eta(n+1)}} \left\{ \sum_{k=n+1}^{3n} \left(\tilde{a}_k \cos(k\eta\tau) + \tilde{b}_k \sin(k\eta\tau) \right) \right\}. \tag{7}$$

For the decision, whether a solution is an artifact or not a relative error $\tilde{e}$ is introduced as

$$\tilde{e} = \frac{\hat{e}}{\hat{x}}. \tag{8}$$

With respect to the demonstration of some results, the same parameters as used in [9]

$$D = 0.06, \varepsilon = -0.1 \text{ and } f = 0.2 \tag{9}$$

are taken, but displayed by $\hat{x}$ (6) and by using a specific labeling. For this, the obtained solutions are first examined with respect for their relative error $\tilde{e}$ (8). Solutions with relative errors larger than 1% are marked by triangles. Solutions with relative error lower than 1% are investigated via Floquet theory for stability and corresponding results are marked with grey circles in the case of unstable and black circles in the case of asymptotically stable solutions. Corresponding results are shown in Figures 1-4 for increasing ansatz orders n.

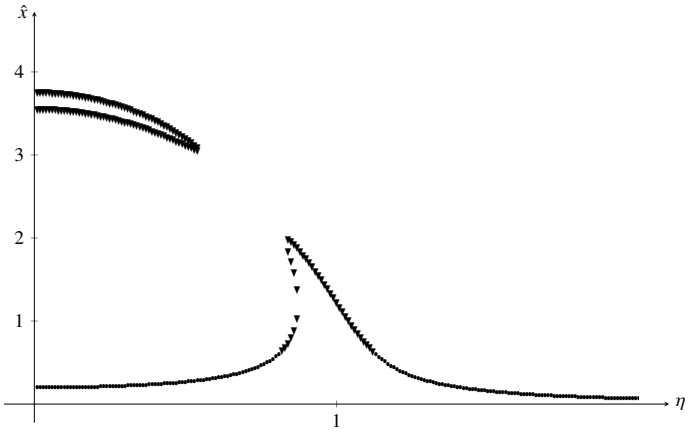

Figure 1. Solutions $\hat{x}$ according to (6) for the Duffing oscillator (2) with Harmonic Balance ansatz (3) in case of $n = 1$. Solutions with relative error $\tilde{e}$ according to (8) larger than 1% are marked by triangles. Solutions with relative error $\tilde{e}$ lower than 1% are marked by circles in grey color in the unstable case (not present in the actual figure) and circles in black color in the asymptotically stable case.

There are two areas of solutions. First the well-known resonance curve starting for small η

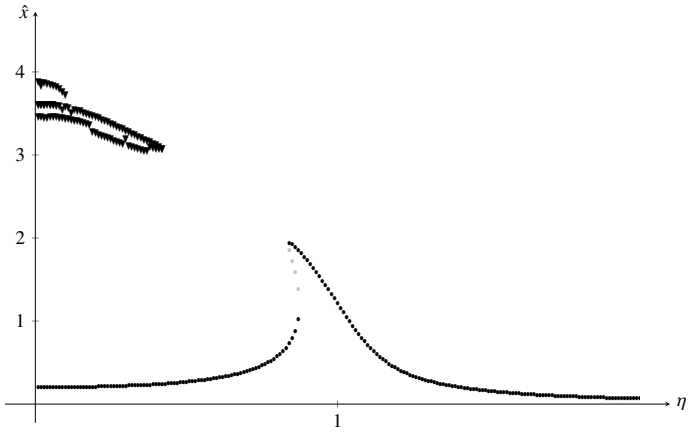

Figure 2. Solutions $\hat{x}$ according to (6) for the Duffing oscillator (2) with Harmonic Balance ansatz (3) in case of $n = 3$. Labeling of solutions as in Fig. 1

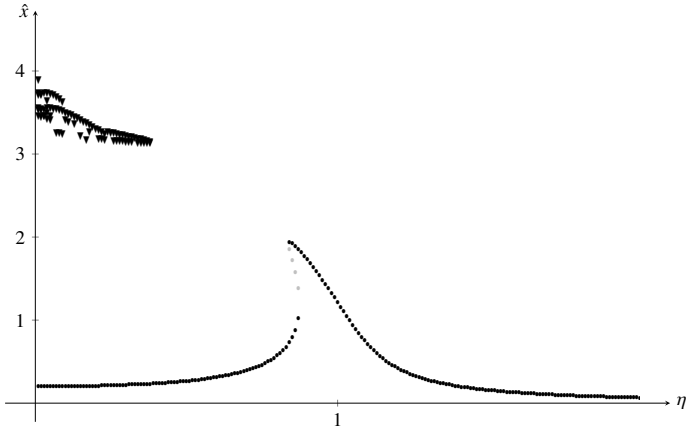

Figure 3. Solutions $\hat{x}$ according to (6) for the Duffing oscillator (2) with Harmonic Balance ansatz (3) in case of $n = 5$. Labeling of solutions as in Fig. 1.

with also small $\hat{x}$, having the resonance peak close to $\eta = 1$ and going to zero for $\eta \to \infty$. Due to the softening characteristic, the resonance peak is turning to the left. This solution preserves its basic shape for all ansatz orders. With the error analysis it can be seen, that this solution shows very small relative errors $\tilde{e}$ for higher ansatz orders and in case of three coexisting solutions for the same η the middle amplitude one is unstable (which is also well known).

The other solutions are the "nose-like" ones occuring for small η and large $\hat{x}$. For $n = 1$, this solution can be found sketched in many textbooks on nonlinear dynamics. They can also occur in case of using perturbation analysis [9]. Increasing the ansatz number, it changes its

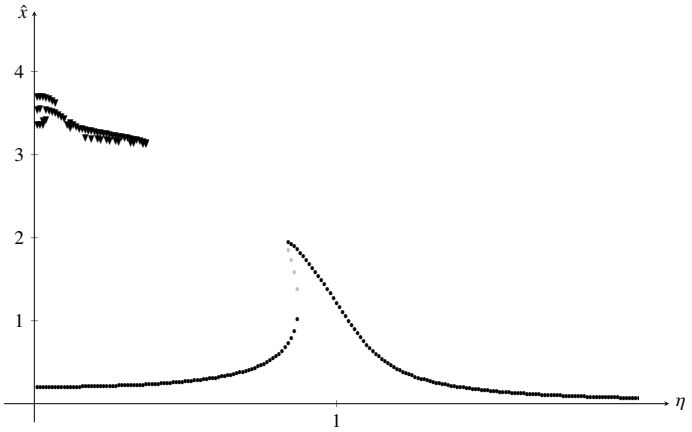

Figure 4. Solutions $\hat{x}$ according to (6) for the Duffing oscillator (2) with Harmonic Balance ansatz (3) in case $n = 7$. Labeling of solutions as in Fig. 1.

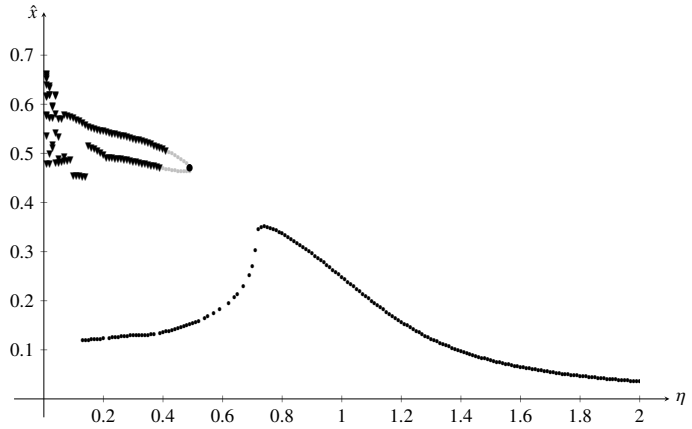

Figure 5. Solutions $\hat{x}$ according to (6) for the Duffing oscillator (2) with Harmonic Balance ansatz (3) in case of $n = 7$. Result from a parameter set investigated by van Dooren [8] with a small separated region with a stable solution. Labeling of solutions as in Fig. 1.

shape (without converging to a final one until $n = 7$) and the error remains large. Therefore we consider this solution to be an artifact solution. In general, solutions with large relative errors even for high ansatz orders are considered to be artifacts in the following. The change of solution shape is also characteristic for these artifacts due to our experience.

In [9] it was furthermore shown, that an additional unstable solution (not being an artifact) with non-zero mean value can be calculated also for small η. To get this solution

as a result of Harmonic Balance, the ansatz (3) has to be extended by a constant term a_0. Finally for this introductory chapter it should be mentioned, that not all parts of the nose-like solution are in any case an artifact. Van Dooren [8] investigated the Duffing oscillator with the parameter set

$$D = 0.2, \varepsilon = -4 \text{ and } f = 0.1105 \tag{10}$$

also using the error criterion by Urabe et al. [7] and focusing on the transition to chaos. Using for this parameter set the same analysis as before it can be seen in Figure 5 for $n = 7$ that small parts of the nose-like solution are not an artifact and that even a small part of this solution is asymptotically stable. This could also be confirmed by numerical integration.

3. Extended Duffing oscillator

In the following the focus will be, as in the last parameter set, on an example with "island" regions of separated solutions. Therefore we consider a modified Duffing oscillator

$$x'' + 2Dx' + x + \varepsilon_1 x^3 + \varepsilon_2 x^2 x' = f_1 \cos(\eta\tau) + f_2 x^2 \cos(\eta\tau) \tag{11}$$

with the methods introduced in section 2. Herein the same denominations are used as in (2) and the classic Duffing Oscillator where the cubic nonlinearity with parameter ε_1 is complemented by a cubic damping term x^2x' with parameter ε_2 and the harmonic excitation with intensity f_1 is combined with a nonlinear parameter excitation term with constant f_2. Such an equation can e.g. be obtained from piezoceramic continua by adding conservative and non-conservative terms in piezoelectric coupling and elasticity [6].

The parameters here are chosen arbitrarily to show certain nonlinear phenomena and do not necessarily represent a real piezoceramic. The same equation of motion is considered in [10] with other parameter sets. Here, the parameters are chosen as $\varepsilon_1 = -0.25$, $\varepsilon_2 = -0.3$, $D = 0.1$, $f_1 = 0.1$ and $f_2 = 0.1$. Using again the ansatz (4), $\hat{x}$ can be calculated according to equation (6) and the relative error $\tilde{e}$ corresponding to equation (8). Corresponding results are shown in Figures 6-9. The results show now three types of solutions for $n = 1$. Beside the well known resonance curve (which shows the well known behavior and converges for higher order n) there is again a nose-like solution for small η and additionally a new island of solutions for medium η i.e. $0 < \eta < 1$. These solutions show initially large errors and change their shape (both regions merge) for higher ansatz orders. Finally for $n = 7$ the right end of the solution island shows low-error but unstable solutions so that again main parts of the results obtained can be considered as artifacts especially the structure observed for $n = 1$.

From discussions of amplitude diagrams of such problems one might be used to, that stable

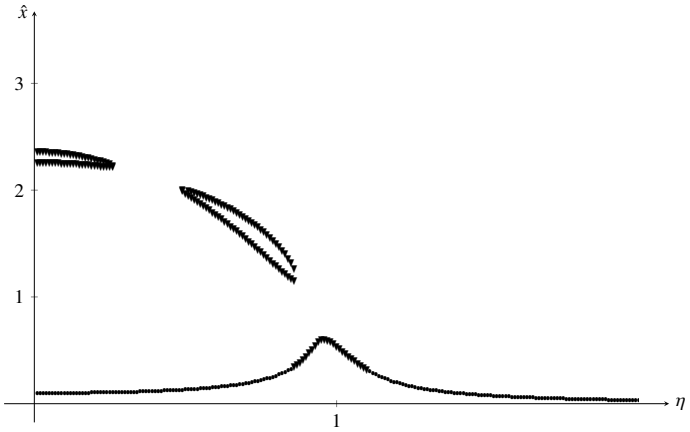

Figure 6. Solutions $\hat{x}$ according to (6) for the extended Duffing oscillator (11) with Harmonic Balance ansatz (3) in case of $n = 1$. Labeling of solutions as in Fig. 1.

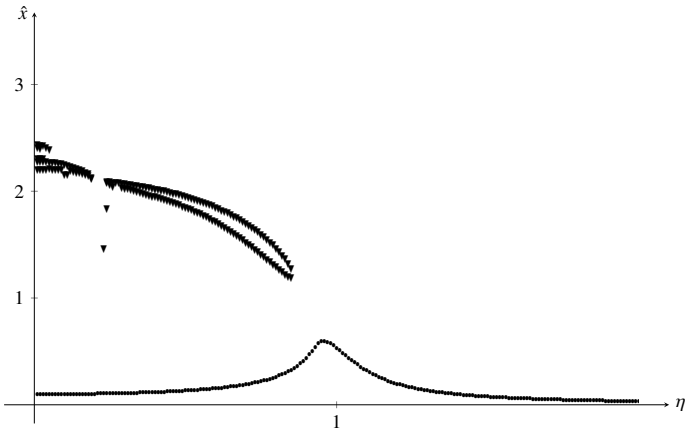

Figure 7. Solutions $\hat{x}$ according to (6) for the extended Duffing oscillator (11) with Harmonic Balance ansatz (3) in case of $n = 3$. Labeling of solutions as in Fig. 1.

and unstable solutions occur in an alternating manner. Therefore, the neighborhood of two unstable solutions might be surprising. In fact, these solutions are in an area of initial conditions showing a fractal character as can be seen in Figure 10 where the basins of attraction are displayed. Hereby, grey points denote initial conditions resulting in the stable solution on the resonance curve. Black points are initial conditions for solutions drifting away to $x \to -\infty$ and white points for $x \to +\infty$. In the immediate neighborhood of these solution, basins of attraction for all three types of solution can be found.

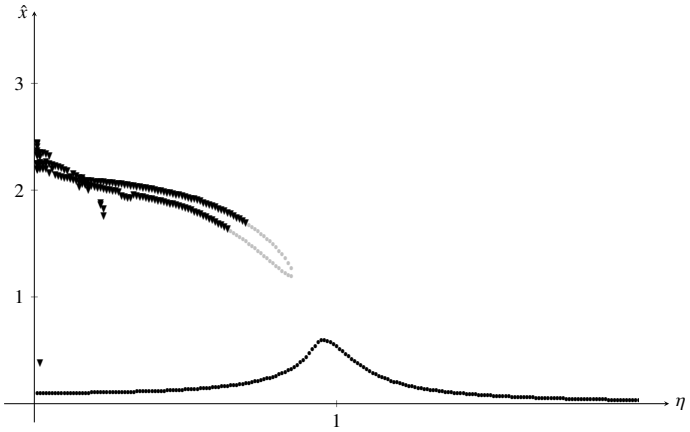

Figure 8. Solutions $\hat{x}$ according to (6) for the extended Duffing oscillator (11) with Harmonic Balance ansatz (3) in case of $n = 5$. Labeling of solutions as in Fig. 1.

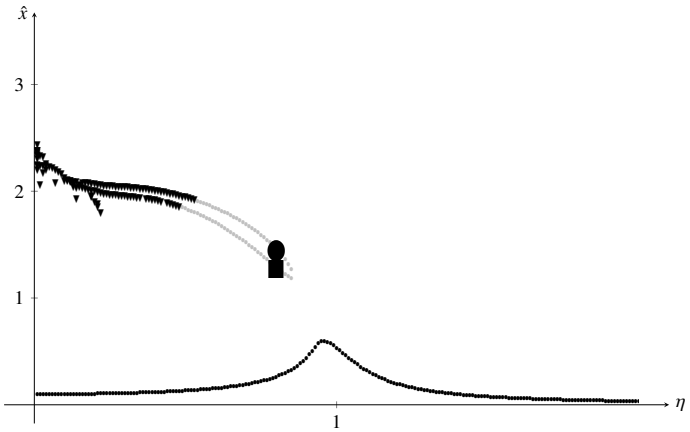

Figure 9. Solutions $\hat{x}$ according to (6) for the extended Duffing oscillator (11) with Harmonic Balance ansatz (3) in case of $n = 7$. Two unstable solutions in the "island" region are marked for $\eta = 0.8$. Labeling of solutions as in Fig. 1.

4. Energy Harvesting

Finally an example from an energy harvesting system shall be discussed in this section. This energy harvesting system consists of a cantilever beam with bonded piezoceramics on the surface close to the clamping. The excitation of the system is realized by a base excitation which may have a harmonic or a stochastic characteristic. In order to increase the energy output, nonlinearities are introduced by mounting two magnets on the frame

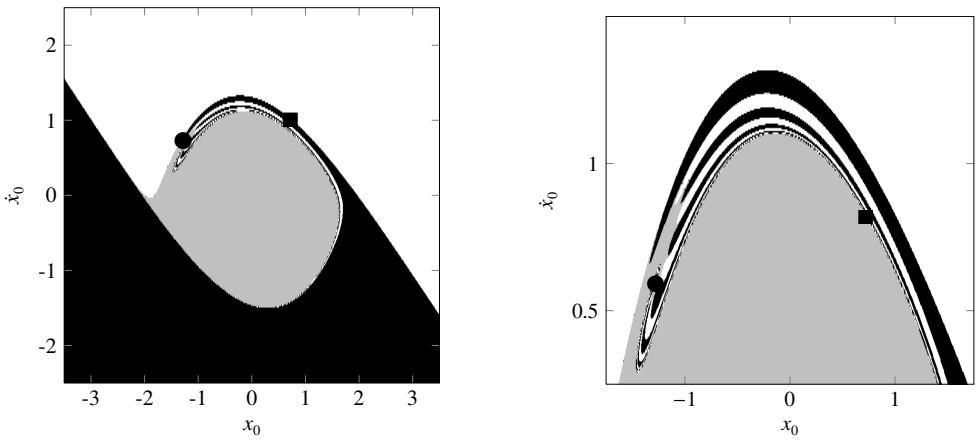

Figure 10. Basins of attraction for $\eta = 0.8$ (left) with detail (right). Grey points denote initial conditions resulting in the stable solution on the resonance curve. Black points are initial conditions for solutions drifting away to $x \to -\infty$ and white points for $x \to +\infty$. Circle and square are marking the initial conditions without transition for the solutions marked in same manner in Figure 9.

the cantilever beam is clamped in close to the tip of the beam. Depending on the magnet properties and positions, multiple stable equilibrium deflections of the beam can result. In our investigations, we are focusing on bistable systems. Corresponding results in case of stochastic excitation can be found e.g. in [5] where probability density functions are calculated. The system also shows a broad variety of solutions if excited harmonically. The simplest useful way of modeling such a system is to discretize the beam with a single mode and couple it with a model of the electric circuit [1], which consist in the present case beside the piezoceramics by a simple resistor. Performing a transformation to dimensionless time τ with circular frequency ω (this is not necessarily the circular eigenfrequency of the mode shape used for discretization) this results in two coupled ODEs namely

$$x''(\tau) + \xi x'(\tau) - \alpha x(\tau) + \beta x^3(\tau) - \chi v(\tau) = f\cos(\eta\tau), \tag{12a}$$

$$v'(\tau) + \lambda v(\tau) = -\kappa x'(\tau). \tag{12b}$$

Herein x is the dimensionless modal coordinate, v is the dimensionless voltage across the resistor, $(\cdot)'$ denotes the derivative with respect to τ and η is the ratio between the excitation frequency and ω. Modal damping is introduced with the coefficient ξ and α and β are the stiffness coefficients which are both strictly positive. χ and κ denote the electro-mechanical coupling coefficients, λ is reciprocal proportional to the product of the capacitance of the piezoce-

ramic layers and the resistance and f is the modal amplitude of the harmonic base excitation. For the following calculations the parameter values $\xi = 0.0105,\ \alpha = \beta = 0.5,\ \chi = -0.1223,\ \lambda = 0.5396,$ $\kappa = -0.2331$ and $f = 0.1739$ are used.

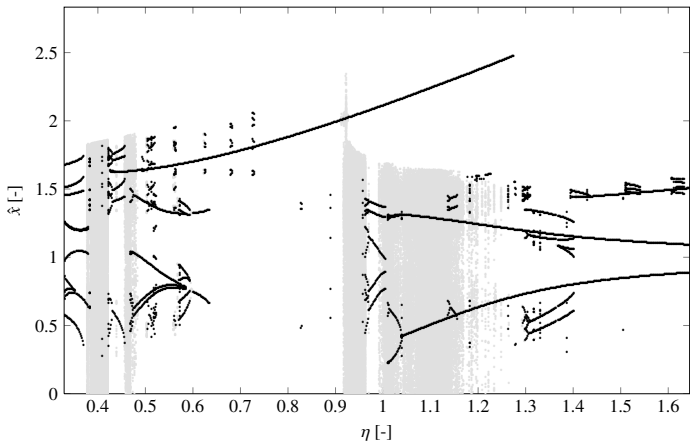

Figure 11. Solutions $\hat{x}$ (turning points of the displacement $x(\tau)$) for the energy harvester (12a), (12b) with numerical integration.

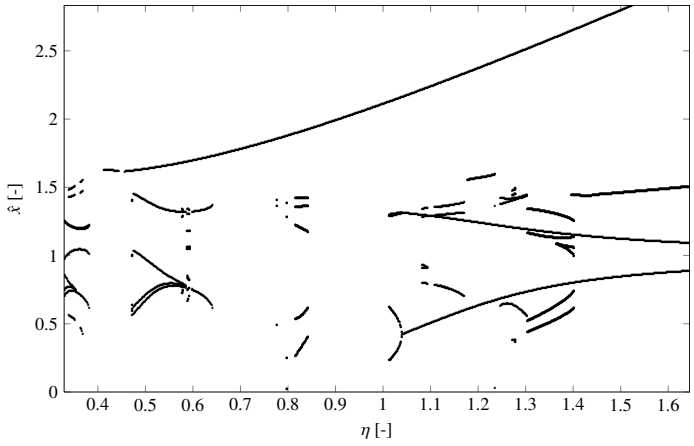

Figure 12. Solutions $\hat{x}$ (turning points of the displacement $x(\tau)$) for the energy harvester (12a), (12b) with Harmonic Balance ansatz (3). Only stable solutions with low relative errors are plotted.

Figure 11 shows results of a numerical integration. In comparison with the Harmonic Balance method of course only stable solutions (and not unstable solutions) can be identified;

but additionally also chaos can be detected. Performing the Harmonic Balance method with the error criterion and displaying only stable solutions, the results in Figure 12 are obtained. It should be mentioned, that the original Harmonic Balance results in numerous additional artifacts and unstable solutions which are neglected in this figure. Both results agree well but the effort for the Harmonic Balance is much lower. For special interest for increasing the energy output of the energy harvester is to obtain so-called interwell solutions, i.e. solutions with vibrations sweeping around both equilibrium positions. Compared to so-called intrawell solutions (vibrations around one equilibrium position) or chaotic solutions these interwell solutions are in general resulting in a higher energy output. In Figure 12 it can be seen, that there is around $\eta \approx 0.75$ an area, where just one interwell solution exists. Such interwell solutions can be identified by the procedure described in this paper in a comparably easy manner. A more detailed discussion of results related to applying the described method to the energy harvester can be found in [4].

5. Conclusions

The classical method of Harmonic Balance in an extended version using an error criterion was applied in the present paper to several nonlinear oscillators. In the error criterion the neglected terms in Harmonic Balance are considered and compared with the remaining terms of the approximate solution. Solutions showing large relative errors even for high ansatz orders are then considered to be artifacts. Solutions with low relative errors are examined for their stability using Floquet's theory. Very often, Harmonic Balance calculations are limited to the ansatz order $n = 1$. With the two examples of a classical and an extended Duffing oscillator it could be shown, that such results may be misleading and that parts of the results could be identified as artifacts. With the example of an energy harvesting system it can be demonstrated that the thereby extended Harmonic Balance is a powerful tool for the rapid identification of interwell solutions promising high energy output.

Acknowledgments

The work on energy harvesting at the Chair of Mechatronics and Machine Dynamics is supported by Deutsche Forschungsgemeinschaft DFG with grant WA 1427/23-1,2.

References

[1] Erturk A., H. J., and Inman, D. J. A piezomagnetoelastic structure for broadband vibration energy harvesting. *Applied Physics Letters*, 96 (2009), 11–14.

[2] Hagedorn, P. *Nichtlineare Schwingungen.* Akademische Verlagsgesellschaft, Wiesbaden, 1978.

[3] Kovacic, I., and Brennan, M. *The Duffing Equation: Nonlinear Oscillators and their Behaviour.* John Wiley & Sons, Ltd, 2011.

[4] Lentz, L., and von Wagner, U. Analysis of a nonlinear energy harvester by the high-order harmonic balance method. *Mechanical Systems and Signal Processing*, submitted (2017).

[5] Martens, W., von Wagner, U., and Litak, G. Stationary response of nonlinear magneto-piezoelectric energy harvester systems under stochastic excitation. *European Physical Journal Special Topics 7*, 222 (2013), 1665–1673.

[6] Parashar, S. K., von Wagner, U., and Hagedorn, P. Nonlinear shear-induced flexural vibrations of piezoceramic actuators: experiments and modeling. *Journal of Sound and Vibration*, 285 (2005), 989–1014.

[7] Urabe, M., and Reiter, A. Numerical computation of nonlinear forced oscillations by Galerkin's procedure. *Journal of Mathematical Analysis and Applications*, 14 (1966), 107–140.

[8] van Dooren R. On the transition form regular to chaotic behaviour in the Duffing oscillator. *Journal of Sound and Vibration 2*, 123 (1988), 327–339.

[9] von Wagner, U., and Lentz, L. On some aspects of the dynamic behavior of the softening Duffing oscillator under harmonic excitation. *Archive of Applied Mechanics 8*, 86 (2016), 1383–1390.

[10] von Wagner, U., and Lentz, L. On artifact solutions of semi-analytic methods in nonlinear dynamics. *Archive of Applied Mechanics*, submitted (2017).

Utz von Wagner, Univ.-Prof. Dr.-Ing.: Chair of Mechatronics and Machine Dynamics, Einsteinufer 5, 10587 Berlin, Germany (*utz.vonwagner@tu-berlin.de*). The author gave a presentation of this paper during one of the conference sessions.

Lukas Lentz, M.Sc.: Chair of Mechatronics and Machine Dynamics, Einsteinufer 5, 10587 Berlin, Germany (*lukas.lentz@tu-berlin.de*).